ASSESSMENT AND DIAGNOSTIC APPLICATIONS OF HEART RATE VARIABILITY

J.H. NAGEL, K. HAN, B.E. HURWITZ, AND N. SCHNEIDERMAN
Behavioral Medicine Research Center,
Departments of Biomedical Engineering and Psychology
University of Miami, Coral Gables, Florida, USA

ABSTRACT

Variations of heart rate (HR), as a normal physiological phenomenon, reflect the activities of the cardiac control system. Various components of heart rate variability (HRV) can be identified by spectral analysis. They are related to different cardiac control activities such as blood pressure, thermal regulation and respiration. Sympathetic and parasympathetic origins have been identified for specific spectral components. Analysis of HRV can provide information on autonomic functions, especially the parasympathetic control of the heart. HRV has also been used to index central nervous system cholinergic functioning reflecting cognitive processes such as attention. Major clinical applications are the assessment of autonomic neuropathy in diabetics and fetal monitoring.

HR is a discrete signal which is not defined between heart beats, and its single values are separated by irregular intervals. Analysis of HRV often requires its representation by a continuous function which produces data that can be regularly sampled. The description of HR in terms of instantaneous frequency of an integral pulse frequency modulator leads to new methods to obtain suitable continuous representations of HR.

Spectral analysis of HRV reveals characteristic patterns; however, overlapping of components reflecting different physiological processes prevents simple decomposition. Assessment of specific cardiovascular regulatory mechanisms requires models representing their influence on heart rate and the acquisition of characteristic reference signals. Thus, decomposition of HRV by adaptive filtering has been developed to reveal numerous cardiovascular parameters such as respiratory sinus arrhythmia (RSA) and estimates of cardiac vagal tone.

Quantitative determination of the various HRV components is limited by the decomposition techniques used. For the commonly applied spectral analysis of HRV, an estimate of cardiac vagal input has been defined as the variance of those HRV components correlated with respiration, an index based on mean values at the expense of information on dynamic changes. However, a continuous measure for RSA is given by the radius vector of the complex representation of RSA obtained by a Hilbert transform, which permits continuous assessment of autonomic cardiovascular regulation. Both human and animal experiments support the validity and diagnostic potential of the described analysis of HRV.

Biomed Eng Appl Basis Comm, 1993 (Apr); 5: 147-158
Keywords: Heart rate variability (HRV), Cardiovascular parameters.

INTRODUCTION

Though heart rate (HR) is one of the basic parameters in medical diagnostics, precise and reliable assessment of its variability is still an engineering and physiological challenge. Measurement of HR and its changes over time, as in a stress test, is a routine diagnostic procedure to evaluate the cardiovascular condition of a patient. Prenatal monitoring, with its unique problems regarding noninvasive acquisition of reliable fetal data, heavily relies on diagnostic HR analysis. The patterns of heart rate oscillations (Fig. 2), and especially the patterns of labor related heart rate fluctuations (Fig. 3), serve to indicate the fetal condition [1,2,3]. Other clinical applications include the assessment of autonomic neuropathy in diabetics (Fig. 4) and intensive care monitoring. The basis for the diagnostic application of HR measurements is the fact that the heart rate variability (HRV) reflects the activities of the cardiac control system. Various components of the HRV can be identified by spectral analysis. They are related to different cardiac control activities such as blood pressure, thermal regulation and respiration [4]. Sympathetic and parasympathetic origins have been identified for specific spectral components [5]. Under resting conditions, spectral analysis of HRV yields three peaks (Fig. 1): a low frequency peak at. 01.05Hz, a mid frequency peak at. 07.15Hz, and a 'high' frequency peak at. 15.5Hz [6]. Since normal respiration frequency is about. 2Hz, the variation in HR due to respiration is reflected by the high frequency peak of the HRV spectrum. Vagal pharmacologic blockade abolishes the mid frequency and high frequency bands [5], whereas sympathetic beta-blockade decreases the low and mid frequency band, indicating that only the high frequency band reflects parasympathetic cardiac input [7]. Thus, analysis of HRV can provide information on autonomic function, especially the parasympathetic control of the heart [8,9,10,11].

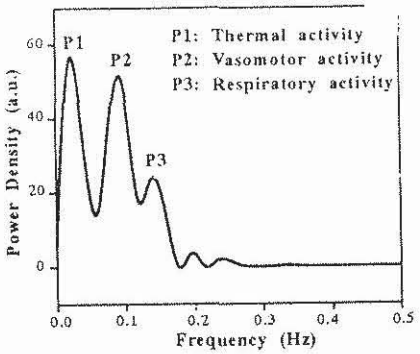

Figure 1: *Typical power spectrum of HR. reflecting the influences of thermal, motor and respiratory control.*

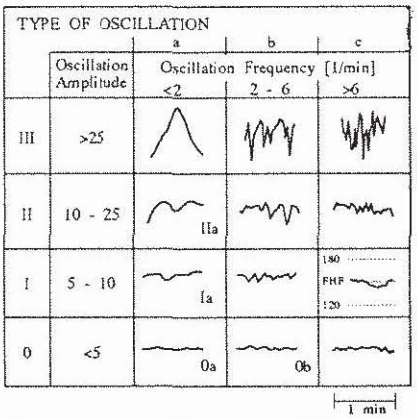

Figure 2: *Classification of FHR Oscil lations according to Hammacher [12].*

Although it is a simple task to determine HR either as a mean value by counting the number of heart beats in a given time interval, or as an instantaneous value by measuring and inverting the interbeat intervals, difficulties arise as soon as non-static situations or transient responses are considered where the required time resolution of the HR curve is smaller or of the same order of magnitude as the interbeat intervals. The question is, how to obtain a value for HR or even an estimate of the cardiac control activities between heart beats, where the HR curve as an inherently discrete signal is not defined. The control activities can definitely not be assumed to be constant during the interbeat intervals. Furthermore, how can the influence of the various parameters which determine the HR be isolated and quantified?

Solutions to these problems, especially the analysis of HRV, require the representation of HR by substitute continuous function of time. A novel method for finding adequate continuous functions will be described in the first section of this paper.

Arrived: June. 15, 1992; accepted: Nov. 24, 1992
Joachim Nagel, Ph. D., Department of Biomedical Engineering University of Miami P.O. Box 248294 Coral Gables, FL 33124 U.S.A.

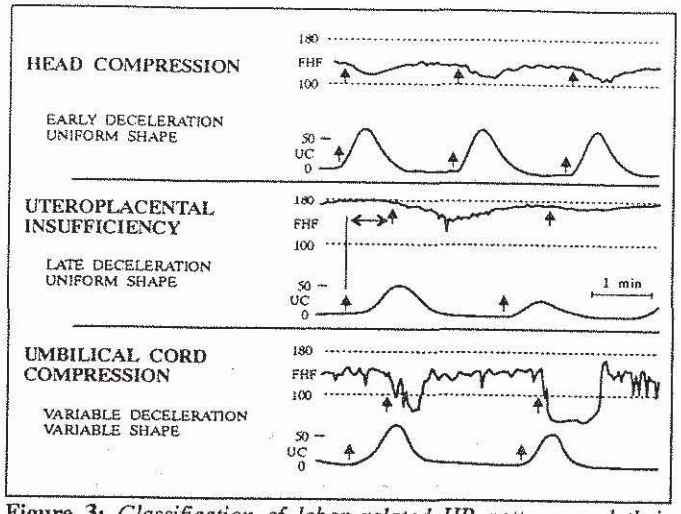

Figure 3: *Classification of labor related HR patterns and their diagnostic interpretation according to Hon [1].*

The continuous representation of HRV will be used for the separation of HRV into its characteristic components, such as the heart rate fluctuations caused by respiration, called respiratory sinus arrhythmia (RSA).

Finally, the paper will deal with the problem of HRV quantification. The HRV signal, in this paper, will represent the HR fluctuations around the mean HR value. Common procedures for the measurement of the magnitude of HRV are to determine the difference between maximum and minimum value of HR within a given time interval, i.e. the peak-to-peak value of HRV, or to determine the signal power of the HRV signal within the interval. This simple analysis, however, does not provide any dynamic information, i.e. information on short term variations of HRV. In the case of RSA, no knowledge can be extracted from this measure about the transitions between inspiration and expiration. A technique will be presented which is able to determine a continuous quantification of HRV, i.e. an instantaneous HRV, which allows exact, high resolution tracing of RSA and provides a continuous estimation of vagal cardiac input.

CONTINUOUS REPRESENTATION OF HEART RATE

Analysis of HRV often requires a continuous representation of the inherently discrete HR measurement. In combination with a suitable cardiac pacemaker model, the cardiac event series can be considered as an irregular sampling of a continuous input to the pacemaker model, m(t). Continuous representation of HR can thus be achieved by a reconstruction of the input function m(t) from the cardiac event series. It should be noted, that m(t) does not represent a continuously interpolated version of the HR signal, but that the analysis of HRV is shifted from the output (measurement of HR) to the input of the system, i.e. the function that causes the HR signal.

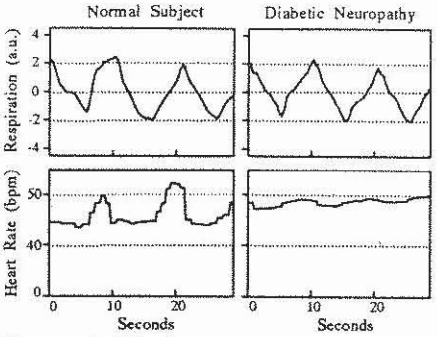

Figure 4: *RSA in a normal subject and a diabetic patient with cardiac autonomic neuropathy during paced respiration.*

A generally used model of the cardiac pacemaker is the integral pulse frequency modulator (IPFM) shown in Fig. 5. The integration is performed on a positive input m(t) representing the autonomic control activity to the heart and an impulse is initiated whenever the integral reaches a threshold T. The integrator is then reset to zero and the integration restarts. This process generates an output impulse train p(t) representing the cardiac event series [13].

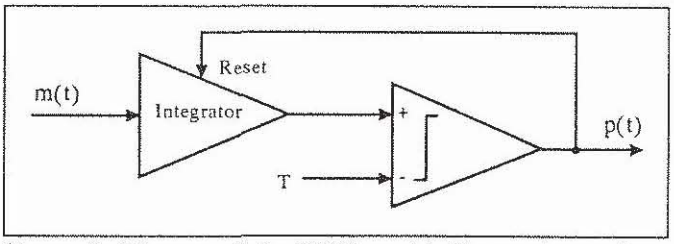

Figure 5: *Diagram of the IPFM model. The continuous input function m(t) is converted into a pulse series p(t). T is the trigger level for the comparator.*

For the cardiac event series p(t), expressed as a sum of unit intensity impulses:

$$p(t) = \sum_k \delta(t - t_k) \qquad (1)$$

the times of any two successive impulses, t_k and t_{k+1}, are related to m(t) by the integral equation:

$$\int_{t_k}^{t_{k+1}} m(t)dt = T \qquad (2)$$

The significance of the IPFM model is that it relates the heart rate with an assumed continuous signal representing the cardiac control activities and, therefore, provides a basis to derive a continuous representation of the heart rate. In other words, the discrete heart rate signal is represented by a continuous signal obtained through the reconstruction of m(t) from the recorded cardiac event series. Two methods to obtain m(t) from the cardiac event series are believed to be consistent with the IPFM model. With the first method, the instantaneous heart rate (IHR) is obtained by constant interpolation of the heart rate in the inter-beat intervals [14]. The IHR signal is a staircase signal with possible discontinuities at each heart beat. With the second method, a low pass filtered event series (LPFES) is computed by:

$$f(t) = \sum_k \frac{\sin(2\pi f_c(t - t_k))}{\pi(t - t_k)} \qquad (3)$$

which is essentially an ideal low pass filtering of the impulse series with the cut-off frequency f_c. It has been claimed that the cardiac event series can be considered as the observation of m(t) in irregular time intervals. Since the mean frequency of these observations is the actual mean heart rate, it follows that, according to the Nyquist criterion, the maximum observable frequency of m(t) is limited to half the mean heart rate, though in reality, the maximum frequency is lower. With a mean heart rate of 60 beats per minute, i.e. 1Hz, the bandwidth of m(t) is always less than 0.5Hz. Therefore, the cut-off frequency fc may be chosen as 0.5Hz [15]. Fig. 6 shows the IHR and LPFES representations of a heart

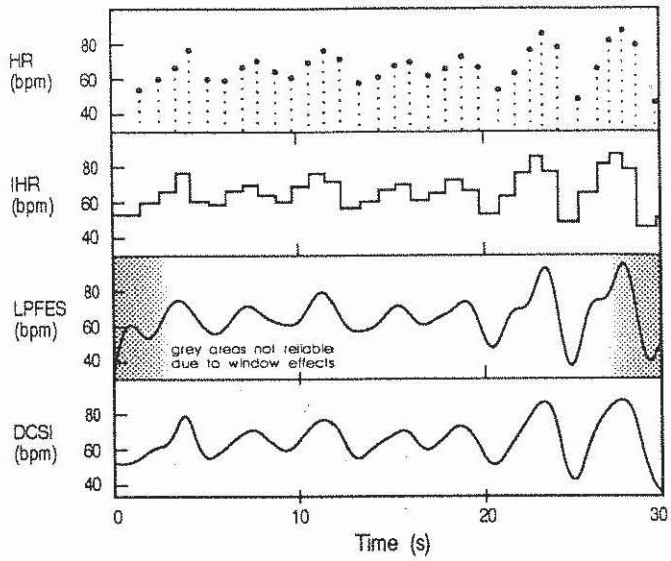

Figure 6: *Three continuous representations of the same HR signal: IHR, LPFES, and DCSI.*

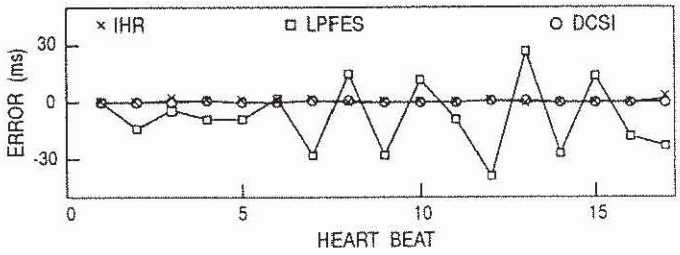

Figure 7: *Timing errors of IHR, LPFES and DCSI for the regeneration of the heart beat impulse series or HR, based on the IPFM model.*

rate signal. According to the IPFM model, a simple test can be performed by computer simulations. Provided that the integrator is reset at the time of a cardiac impulse, an output impulse train will be generated by the IPFM which will be the same as the original cardiac event series, if the calculated m(t) is consistent with the model. As a testing result, Fig. 7 shows the time differences between the impulse train received from m(t) and the true cardiac event series. The IHR signal, though nonphysiological and inadequate for digital signal processing, is consistent with the model since the generated impulse train is virtually the same as the cardiac event series The maximum error is 1 ms, which corresponds to the time resolution of the computer simulations. It is obvious that the impulse train generated from the LPFES is significantly different from the original cardiac event series. Therefore, the LPFES' signal actually is not consistent with the model.

1. Cubic Spline Interpolation

Since there is only one heart rate value corresponding to each inter-beat interval regardless of the duration of the period information concerning heart rate is inherently discrete. To obtain a continuous representation, some kind of interpolation between known samples of m(t) should be used. The first problem is to find the samples. According to Eq. 2 and the mean value theorem, one can conclude that if m(t) is continuous in the period (t_k, t_{k+1}), there exists at least one t_ξ for which:

$$m(t_\xi)\ (t_{k+1} - t_k) = T \qquad t_k \le t_\xi \le t_{k+1} \tag{4}$$

For the case of the IHR method, m(t) is assumed to be constant during each inter-beat interval, so there is no need to identify t_ξ; In the more general case, where m(t) is not limited to a constant t_ξ is unknown. As a consequence, no sample points for m(t) are readily available. Fortunately one can express Eq. 2 in terms of M(t), the continuous integral of m(t). Let $t_o = 0$ be the time origin, then an equivalent expression for Eq. 2 is:

$$M(t_k) = \int_0^{t_k} m(t)\ dt = kT \tag{5}$$

As a function of time, the values of M(t) at t_k, k = 1, 2, ..., n are given by kT. From these given points, M(t) can be reconstructed by interpolations and m(t) can be obtained by calculating the derivative of M(t). If M(t) is obtained by piece wise linear interpolations, its derivative is equal to the IHR signal. Although M(t), in this case, is continuous at the joints, its derivative m(t) is not. To provide continuity to its higher order derivatives at the joints, cubic spline interpolation may be considered.

The spline interpolations are piece-wise polynomial interpolations in which low degree polynomials are chosen to pass each pair of given points and provide the maximum smoothness at joints. Cubic spline interpolation can provide continuity at joints up to the second order derivatives. As a widely used tool in engineering practice, the method of computing cubic spline interpolation has been well established. Because there is no information available outside the recording period, i.e. the first derivatives of M(t) for the first and last points are not known, free-end cubic splines are used for the interpolation of M(t). The two second derivatives at both ends required by the algorithm may be set to zero, provided that the trends of m(t) do not change at both ends of the period. After the spline functions are obtained, the derivation can be performed on these functions and the interpolations of m(t), instead of M(t), can be computed directly. The signal derived this way may be called the derivative of cubic spline interpolation (DCSI). In summary, the procedure for the new method is:

(1) Obtain the cardiac event series with a total of n + 1 beats in the record occurring at $t_0, t_1, \ldots, t_n$ with $t_0 = 0$.

(2) For the defined points $M(t_k) = kT$, k = 0, 1, ..., n and with the two second order derivatives at both end points equal to zero, calculate the coefficients of the n free-end cubic splines $C_i(t) = \alpha_i + \beta_i (t - t_i) + \gamma_i (t - t_i)^2 + \delta_i (t - t_i)^3$, with i = 0, 1, ..., n - 1, for the n intervals between consecutive points.

(3) With the derivatives $C_i'(t)$ of the cubic splines, m(t) is:

$m(t) = \sum C_i'(t)\ [u(t - t_i) - u(t - t_{i+1})]$ where $C_i'(t) = \beta_i + 2\gamma_i(t - t_i) + 3\delta_i(t - t_i)^2$, for $t_i \le t \le t_{i+1}$, i = 0, 1, ..., n - 1, and u(t) is the unit step function.

2. Coefficients of Free-End Cubic Splines

Given n + 1 points $\{t_i, x_i\}$, i = 0, ..., n, and two second order derivatives at both end points: $2q_o$ and $2q_n$, the n free-end cubic splines:

$$C_i(t) = \alpha_i + \beta_i (t - t_i) + \gamma_i (t - t_i)^2 + \delta_i (t - t_i)^3$$

can be computed as following:

With $\Delta t_i = t_{i+1} - t_i$

$\Delta x_i = x_{i+1} - x_i$

and $\Delta s_i = \Delta_{xi} / \Delta t_i$

Calculate $q_1, \ldots, q_{n-1}$ by solving the (n - 1) system of linear equations:

$$\begin{cases} \Delta t_0\ q_0 + 2(\Delta t_0 + \Delta t_1)q_1 + \Delta t_1\ q_2 = 3(\Delta s_1 - \Delta s_0) \\ \Delta t_1\ q_1 + 2(\Delta t_1 + \Delta t_2)q_2 + \Delta t_2\ q_3 = 3(\Delta s_2 - \Delta s_1) \\ \quad \cdot \\ \quad \cdot \\ \Delta t_{n-2} q_{n-2} + 2(\Delta t_{n-2} + \Delta t_{n-1})q_{n-1} + \Delta t_{n-1} q_n = 3(\Delta s_{n-1} - \Delta s_{n-2}) \end{cases}$$

Note that q_o and q_n are given parameters. Then the

coefficients of the cubic splines for each interval can be obtained from the following formula:

$$\alpha_i = x_i$$
$$\beta_i = \Delta s_i - \Delta t_i\,(2q_i + q_{i+1})/3$$
$$\gamma_i = q_i$$
$$\delta_i = (q_{i+1} - q_i)/3\Delta t_i$$

3. Results

A DCSI representation of the heart rate is shown in Fig. 6. The DCSI signals were tested by simulations and a result is shown in Fig. 7. Similar to the IHR, the impulse trains from the DCSI signals are almost exactly the same as the recorded signals with a maximum error of 1 ms, which is the resolution of computer simulation used. In addition to this consistency with the IPFM model, the DCSI representation is continuous as shown in Fig. 6. Regularly sampled data representing HRV are readily obtained, and a variety of digital signal processing techniques may be applied for the analysis of HRV. Whether the given solution of cubic spline interpolation is an adequate representation of the physiological situation depends, of course, on the validity of the IPFM model itself, which will be discussed later on in this paper.

DECOMPOSITION OF HEART RATE VARIABILITY

Several researchers have reported that phasic changes in respiration have a gating influence on cardiac vagal efferent activity such that during the expiratory phase of respiration a slowing of HR is observed [16]. The oscillatory influence of respiration on HR has been referred to as RSA. The magnitude of the HRV within the spectral range of respiration has been used as a measure of the strength of parasympathetic activity of the autonomic nervous system [17,18]. In addition, RSA has also been employed to index central nervous system cholinergic functioning reflecting cognitive processes such as attention [19].

Spectral analysis has been used to partition the HR variation occurring at the respiratory frequencies [18,20]. The spectrum of HR clearly shows a peak at the frequency of respiration (see Fig. 8), it contains, however, also prominent frequency bands which are not related to respiration [5]. These findings suggest that in addition to HRV reflecting vagal cardiac influences, sympathetic and non-neural factors may contribute to the production of HRV [5,20]. Spectral analysis enables the quantitative description of RSA over a specified period. This procedure, however, limits the assessment to prolonged periods of stable physiological conditions requiring stationarity of means and variances of the signals collected. This limitation prohibits a beat-by-beat assessment of vagal activity, which is desirable in studies examining dynamic cardiorespiratory responsiveness to challenge conditions. Furthermore, spectral overlapping of different components of HRV, as e.g. the respiration, blood pressure, and temperature bands (Figs. 1 and 8), leads to considerable errors. Therefore, in the present study we have attempted to develop a methodology to:

1) quantitate the magnitude of respiratory (RSA) and nonrespiratory (NRSA) influences on HRV;
2) provide RSA and NRSA measures which are insensitive to overlapping of spectra; and
3) provide the capability for deriving a continuous beat-by-beat assessment.

The difficulties with the power spectrum analysis is, that all phase information in HRV is lost. This means, that two components of HRV occupying the same spectral band, but with different phase distributions cannot be separated. To improve the situation, a

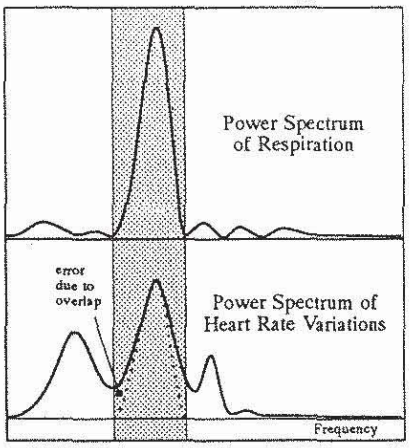

Figure 8: *Spectral estimation of RSA as the area under the HR spectrum in the range of respiration.*

technique must be developed which retains the phase information and separates the single components by correlation of HRV with the parameter of interest, e.g. respiration, or labor, referring to fetal monitoring. A solution for the adequate, continuous separation of HRV components could be found by developing an adaptive filter for the decomposition of HRV in the time domain.

1. Adaptive Filtering

Adaptive filtering is a technique originally developed for estimating signals corrupted by additive noise or interferences [9]. The method uses a primary input containing the desired signal superimposed by additive noise, and a reference input containing the noise which is correlated in some unknown way with the noise in the primary input. The reference input is adaptively filtered and subtracted from the primary input to obtain the best estimated signal. Fig. 9 shows the block diagram of an adaptive filtering system. The primary input d(t) is considered to consist of two uncorrelated components v(t) and s(t), and v(t) is correlated with the reference input x(t) while s(t) is not. The reference input x(t) is processed by an adaptive filter with adjustable coefficients and its output is r(t). The system output n(t) is obtained by subtraction of r(t) from d(t). By feeding the output signal n(t) back to the adaptive filter and adjusting its coefficients, the mean square error of the system $E(n(t) - s(t))^2 = E(v(t) - r(t))^2$ can be minimized. Therefore, n(t) is the best estimate in the least square sense to s(t), and at the same time, the r(t) is the best estimate of v(t). Adaptive filtering before subtracting allows the treatment of input signals that are deterministic or stochastic, stationary or time variable. According to the model described by Womack [21], the HRV signal has two distinct and uncorrelated components, RSA, which is correlated with respiration, and the fluctuations due to other influences. Therefore, adaptive filtering can be readily applied to analyze HRV signals. Taking the HRV signal as primary input d(t), with v(t) representing RSA and s(t) representing other variations, and the simultaneously recorded respiratory signal as reference input x(t), the two component signals v(t) and s(t) will be best estimated by the adaptive filtering system outputs r(t) and n(t), respectively. As a result, the HRV signal is partitioned into r(t), an estimate of RSA, the component due to respiration, and n(t), an estimate of fluctuations due to other influences.

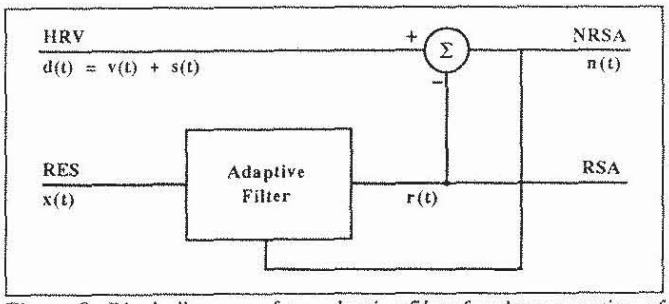

Figure 9: *Block diagram of an adaptive filter for the separation of RSA from HRV.*

2. Implementation of the Adaptive Filter

The adaptive filtering system for the analysis of HRV signals has been implemented on a digital computer (PS/2) using the least mean square (LMS) algorithm [22]. As input function for HRV, the representation by a continuous cubic spline is chosen as described in the previous section of this paper. A respiration signal is obtained using a mercury strain gauge fastened on the subject's chest. Both HRV and respiration signals are digitized with a sampling rate of 4Hz.

The reference input vector X_i and filter coefficient

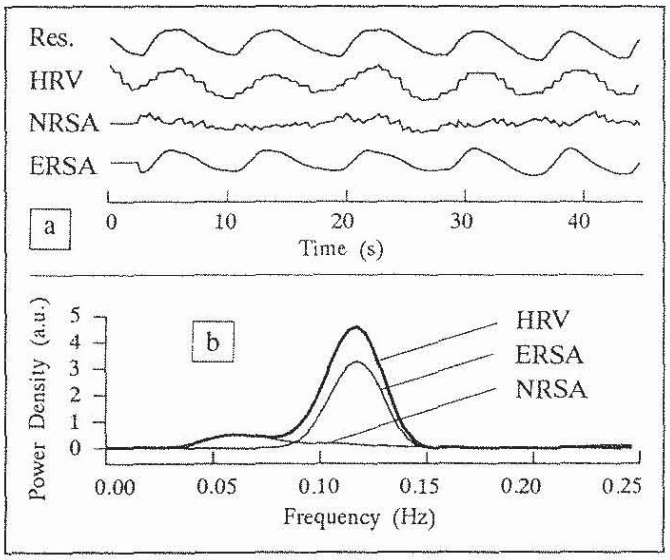

Figure 10: *Decomposition of HRV using the adaptive filter. (a) Res. - respiration; HRV - heart rate variability; NRSA -estimated non respiratory fluctuations; ERSA - estimated respiratory fluctuations; (b) Power spectra of HRV, NRSA and ERSA.*

vector W are defined as:

$$X_i = [x_i, x_{i-1}, \ldots, x_{i-p}]^T$$
$$W = [w_0, w_1, \ldots, w_p]^T$$

where p is the order of the filter. The filter output r_i and system output n_i are:

$$r_i = X^T_i W = W^T X_i$$
$$n_i = d_i - r_i$$

According to the LMS algorithm, the filter coefficients are updated by:

$$W_{i+1} = W_i + 2\mu n_i X_i$$

where W_{i+1} and W_i are next and present weight vectors, respectively, μ is the factor that controls stability and the rate of convergence. It has been shown that with arbitrary initial weights, the algorithm will converge to its mean and remain stable as long as the parameter μ is:

$$\mu_{max} > \mu > 0$$

where μ_{max} is reciprocal of the maximum eigenvalue of the reference auto-correlation matrix [22]. Since the algorithm is based on the steepest descent method and actually makes use of gradients of mean-square error (MSE) functions in searching the optimal solutions, the average excess MSE, in processing time varying signals, consists of two components due to gradient noise and weight vector lag. With the μ satisfying the convergence condition, the former is proportional to μ while the latter is inversely proportional to μ. The larger μ, the faster the convergence and therefore the smaller the tracking error due to lag. However the larger μ will result in larger gradient noise. The optimal values for parameters p and μ are problem dependent [23].

For the analysis of HRV signals, we use p=10 and μ=0.005 at a sample rate of 4Hz. Fig. 10(a) shows a decomposition of a real HRV signal by the adaptive filtering system. ERSA represents the estimated HR fluctuations correlated to respirations and NRSA represents the estimated non-respiratory HR fluctuations.

3. Performance Test

The performance of the system was tested using artificial test signals which were generated according to a simple HRV model. Figure 11 demonstrates the process. The NRSA component was simulated using a sinusoid with a frequency of 0.1Hz and corrupted by random noise. The respiration signal was simulated by a 0.19Hz sinusoid with its amplitude partially modulated by another very low frequency (0.01Hz) and a random phase sinusoid which is simulating a time varying process in respiration. The RSA component was obtained by passing the respiration signal through a low-pass filter, and the HRV signal was formed by adding NRSA and RSA components.

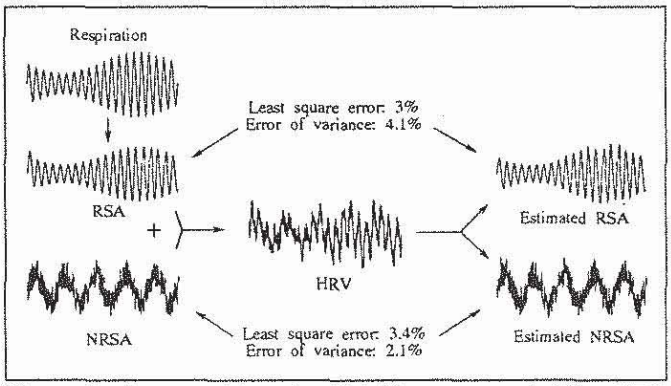

Figure 11: *Decomposition of artificial heart rate variability (HRV) signals using the adaptive filter.*

First, the precision of waveform estimation was tested. The NRSA and RSA components were considered as waveforms to be estimated using the adaptive filtering system. After the estimated waveforms were obtained, they were compared with the known components and the normalized least square errors (LSE) were calculated. The average LSE for NRSA and RSA component estimations obtained from 10 sets of test signals were 3.4% and 3%, respectively.

Next, the precision of variance estimations was analyzed. After the estimated signals were obtained, their variances were calculated and compared with corresponding variances of the true components. The average relative errors in estimating variances of NRSA and RSA components for the same sets of test signals were 2.1% and 4.1%, respectively.

ESTIMATES OF CARDIAC VAGAL TONE

Since RSA is primarily mediated through the vagus nerve, the measurement of RSA can be used as an index of cardiac vagal tone [16]. One measure of RSA, which

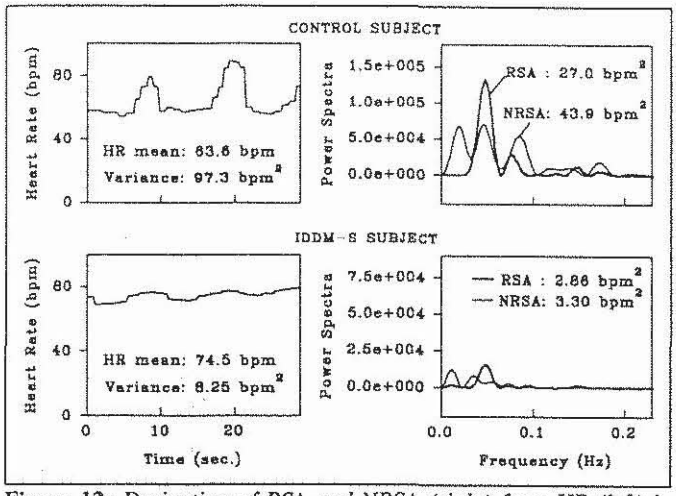

Figure 12: *Derivation of RSA and NRSA (right) from HR (left) in a healthy control subject and an insulin dependent diabetes mellitus patient (paced respiration).*

was originally obtained in the frequency domain using the so-called V-hat procedure (see Fig. 8), is the variation of the HRV signal falling into the spectral band of respiration [17,18,24]. By decomposing HRV using the adaptive filter, the signal describing the fluctuations due to respiration can be obtained. The variance of this signal represents the estimate of cardiac vagal tone (ECVT), and is readily calculated. As a time domain approach, it is simple, fast and robust. Compared to the V-hat procedure, the advantages are:

(1) capability of continuously tracking time varying signals in HRV analysis while these signals are treated as stationary in the spectral analysis approach. The precision of estimation is improved. Following the V-hat procedure (spectra calculated via Fast Fourier Transform (FFT) and Hamming window) to estimate variances of RSA components of test signals, even in cases where the RSA and NRSA components are well separated in the spectra, the average relative error obtained was about 20%. The error for the same measurement using the time domain approach was reduced to 4.1%.

(2) capability of separating uncorrelated components with overlapping spectra. Since the decomposition using adaptive filtering is performed based on the correlations with respiration, overlap of the two component spectra are allowed. Figs. 10(b) and 12 show spectra of a real HRV signal and its two component signals obtained using adaptive filtering. The spectra of the component signals partially overlap. In contrast to the V-hat procedure, the adaptive filter does not require arbitrary decisions of bandwidth boundaries in the HRV spectrum thus eliminating this factor as a source of error in the estimation of cardiac vagal tone.

Measurement of RSA

RSA is observed as the heart rate changes associated with respiration. The heart rate increases with inspiration and decreases with expiration. Different methods have been used to measure these changes. Most of them can be summarized as indices of amplitude or variation. A simple and straightforward measurement is the determination of difference between the maxima and minima of HR or the interbeat intervals (IBI). Quantified as peak-to-peak difference of excursion of the IBI signal, an index called VHP (variations of heart period) was shown by Katona to be proportional to the parasympathetic control of the heart [9]. Hirsch and Bishop performed a systematic investigation of RSA in humans by means of quantifying RSA as the breath-by-breath heart rate changes [27]. The advantage of this index is its simplicity in terms of understanding and measurement. More complex statistical measures for RSA have been published, such as variation and mean square successive differences, which is currently used in diagnosing diabetic neuropathy [25]. Since the measurement is performed on the HRV signal rather than the RSA signal, post measurement statistical corrections, e. g. averaging, are usually required to increase the precision of the results and reduce errors due to non-respiratory influences on HR.

According to Parssevel's theorem, a power spectrum represents a distribution of total variance of a zero mean signal. Based on this theorem, frequency domain techniques have been used for the decomposition of HRV variance and quantitation of RSA. Since RSA represents the fluctuations of HR due to respiration, it can be expected that the spectrum of the RSA component in HRV and the spectrum of a measured respiration signal appear in the same frequency band and show some similarity. Therefore, a measure of RSA, based on the power spectral densities of HRV and respiration, has been defined as the sum of the power spectral density components of HRV in the spectral range of respiration

[18]. The result of this estimate is a variation index. This becomes clear by considering an RSA signal which has only spectral components within the respirational frequency band. The summation of its power spectrum is equal to the variance of the signal in the time domain. The drawback of this variation index is, that it represents an average value and that in almost all cases overlap of spectral components in the HRV prevent simple isolation of the spectral components related to respiration.

Though the difficulties with spectral overlap can be solved by the adaptive filtering technique described earlier in this paper, there is no means of obtaining instantaneous instead of averaged values. Such an instantaneous, continuous measure of RSA can be obtained by calculating the envelope of the complex representation of the RSA signal which is obtained by a Hilbert transform. This estimate permits the analysis of dynamic changes of autonomous cardiovascular regulation.

Measuring oscillatory changes of a signal means obtaining its envelope. The envelope of a signal can be calculated as the magnitude of its analytic complex representation obtained by a Hilbert transform. For a real signal in the form:

$$s(t) = a(t)\cos(\phi(t))$$

where a(t) represents the envelope and $\phi(t)$ the phase. Provided the spectra $F\{a(t)\}$ and $F\{\cos(\phi(t)\}$ do not overlap, then [26]:

$$a(t)\cos(\phi(t)) + jH\{(a(t)\cos(\phi(t))\} = a(t)\cos(\phi(t)) + ja(t)\sin(\phi(t))$$

$$a(t) = \{[a(t)\cos(\phi(t))]^2 + [a(t)\sin(\phi(t))^2\}^{1/2} \quad (6)$$

In practice, the Hilbert transform based analytic signal can be calculated via fast Fourier transforms (FFT). After calculating the Fourier spectrum of a given real signal, its positive harmonics are multiplied by 2 and the negative harmonics are set equal to zero. Then, an inverse FFT is performed on the modified spectrum, resulting in the complex analytic representation. The envelope is obtained as the magnitude of this complex signal. Fig. 13 shows an example for the envelope determination.

VALIDATION

One important goal of the previous considerations was to develop a method which would permit continuous monitoring of vagal tone. In order to validate the described solutions, animal experiments have been performed in which HRV and respiration are measured

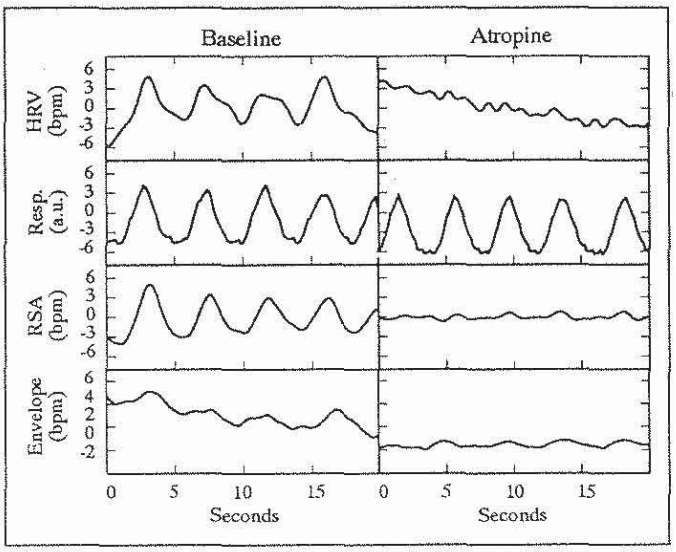

Figure 13: *Estimation of RSA by calculation of its envelope using the complex representation. Baseline and reduction of RSA by atropine in a human subject.*

simultaneously during pharmacological manipulations of vagal activity. Envelopes of RSA are observed during infusions of saline, phenylephrine (which increases blood pressure and produces a reflexive increase in vagal activity), and atropine methylnitrate (which blocks vagal activity at the heart. Preliminary results show that the RSA envelope is sensitive to pharmacological manipulations of vagal activity and therefore appears to be a good non-invasive estimate of cardiac vagal tone.

Assessing autonomic function in humans

To clarify the respective contributions of the parasympathetic and sympathetic nervous system to heart rate variations, we subjected six healthy human volunteers to pharmacologic blockade while resting in the seated position and breathing regularly. Subjects participated in a two day protocol, each day consisting of a resting baseline, followed by an intravenous bolus sa-

line-placebo infusion, followed by another resting baseline and then two drug treatments using either atropine sulfate (0.04 mg/kg, i.v.) or propranolol hydrochloride (10 mg i.v.). The drug treatment was counterbalanced over the two days. Therefore, single and double autonomic branch blockade were employed and RSA and NRSA measures derived using the adaptive filtering method. Fig. 14 displays the change in RSA and NRSA relative to the saline-placebo levels during the pharmacological manipulations. There were significant decreases in RSA during parasympathetic blockade with atropine, which did not significantly differ from the decrease in RSA observed during the double autonomic blockade. This would suggest that the RSA accounts for all the change in heart rate during the double blockade treatment. However, there was also a significant decease in RSA during sympathetic blockade with propranolol, suggesting that with the removal of the sympathetic system, there is either a compensatory decease in parasympathetic cardiac input or that the RSA measure may in part reflect some sympathetic influences. The difference between RSA during sympathetic blockade and during double blockade can be said to reflect the contribution of the vagus to resting heart rate (see Fig. 14).

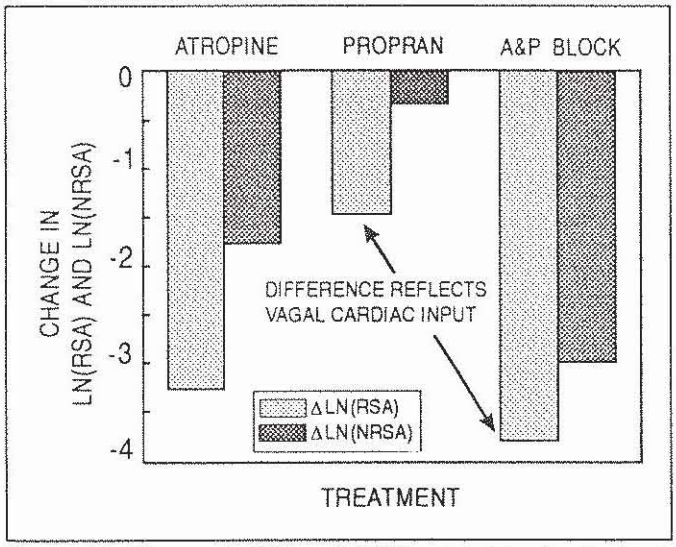

Figure 14: *Changes in RSA and NRSA related to placebo levels during single and double autonomic blockade.*

REFERENCES

1. Hon EH, An introduction to fetal heart rate monitoring Harty Press, New Haven, 1971.
2. Porges SW, Heart rate indices of newborn attentional responsivity. Merrill-Palmer Quarterly of Behavior and Development, Vol. 20, No. 4, 1979.
3. Porges SW, Innovations in fetal heart rate monitoring: the application of spectral analysis for the detection of fetal distress. In: Infants Born at Risk, T. M. Fields et al. (Eds.) New York, ppl7-28, 1979.
4. Sayers BMcA, Analysis of heart rate variability Ergonomics, Vol. 16: ppl7-32, 1973.
5. Akselrod S, Gordon D, Ubel FA, et al., Power spectrum analysis of heart rate fluctuation: a quantitative probe of beat-to-beat cardiovascular control. Science Vol. 213, pp220-222, 1981.
6. Porges SW, and Bohrer RE, The analysis of periodic processes in psychophysiological research. In: J. l Cacioppo and L. G. Tassinary (eds.), Principles c Psychophysiology, Guilford Press, New York, 1990.
7. Weiss F, Heidenreich F, and Runge U, Contributions c sympathetic and vagal mechanisms to the genesis of heart rate fluctuations during orthostatic load: a spectral analysis Journal of the Autonomic Nervous System, 21, ppl27-13 1987.
8. Pomeranz B, Macaulay RJB, Caudill A, et al Assessment of autonomic function in humans by heart rate spectral analysis. Am. J. of Physiol., Vol. 248, (Heart Circ Physiol. 17), ppH151-H153, 1985.
9. Katona PG, and Jih F, Respiratory sinus arrhythmi noninvasive measure of parasympathetic cardiac control. Appl. Physiol., Vol. 39, No. 5, pp801-805, 1975.
10. Bernardi L, Calciati A, Gratarola A, Battistin I, Fratino P and Finardi G, Heart rate - respiration relationship: computerized method for early assessment of cardiac autonomic damage in diabetic patients. Acta Cardiologica, Vol. 41, ppl97-206, 1986.
11. Fouad FM, Tarazi RC, Ferrario CM, Fighaly S and Alocandri C, Assessment of parasympathetic contral of heart rate by a noninvasive method. American

Journal of Physiology, Vol. 246 (Heart Circulation Physiology Vol. 15), ppH838-H842, 1984.

12. Fischer WM, Kardiotokographie. Georg Thieme Verlag, Stuttgart, 1973.
13. Hyndman BW, and Mohn RK, A pulse modulator model of pacemaker activity. Digest of the 10th Int'l Conf. on Med. and Biol. Eng., Dresden, p223, 1973.
14. De Boer RW, Karemaker JM, and Strackee J, Description of heart-rate variability data in accordance with a physiological model for the genesis of heartbeats. Psychophysiology, Vol. 22: ppl47-155, 1985.
15. Hyndman BW, Mohn RK, A model of the cardiac pacemaker and its use in decoding the information content of cardiac intervals. Automedica, Vol. 1, pp239-252, 1975.
16. Katona PG, Poitras JW, Barnett GO, and Terry BS, Cardiac vagal efferent activity and heart period in the carotid sinus reflex. Am. J. Physiol., 218, ppl030-1037, 1970.
17. McCabe PM, Yongue BG, Porges SW and Ackles PK, Changes in heart period, heart period variability, and a spectral analysis estimate of respiratory sinus arrhythmias during aortic nerve stimulation in rabbits. Psychophysiology, 21, ppl49-158, 1984.
18. Porges SW, McCabe PM, and Yongue BG, Respiratory heart rate interactions: psychophysiological implications for pathophysiology and behavior. In: Perspectives in Cardiovascular Psychophysiology, J. T. Cacioppo and R. E. Petty (Eds.), Guilford Press, New York, 1982.
19. Richards JE, Infant visual sustained attention and respiratory sinus arrhythmia, Child Development, 58, pp488-496, 1987.
20. Chess GF, Tam RMK, and Calaresu FR, Influence of cardiac neural inputs on rhythmic variations of heart period in the Cat. Am. J. Physiol., 228, pp775-780, 1975.
21. Womack BF, The analysis of respiratory sinus arrhythmia using spectral analysis and digital filtering. IEEE Transactions on Bio-Medical Engineering, Vol. BME-18, pp399-409, 1971.
22. Widrow B, Glover JR, McCool JM, et al., Adaptive noise cancelling: principles and applications. Proc. IEEE, 63, ppl692-1716, 1975.
23. Widrow B, McCool JM, Larimore MG and Johnson CR Jr, Stationary and nonstationary learning characteristics of the LMS adaptive filter. Proceedings of the IEEE, Vol. 64, ppll51-1162, 1976.
24. Yongue BG, McCabe PM, Porges SW, Rivera M, Kelley SL and Ackles PK, The effects of pharmacological manipulations that influence vagal control of the heart on heart period, heart-period variability and respiration in rats. Psychophysiology, 19, pp426-432, 1982.
25. Ewing DJ, Borsey DQ, Bellavere F, and Carke BF, Cardiac autonomic neuropathy in diabetes: comparison of measures of R-R interval variation. Diabetologia, Vol. 21, ppl8-24, 1981.
26. Boashash B, Estimating and interpreting the instantaneous frequency of a signal - Part 1: Fundamentals. Proceedings of the IEEE, Vol. 80, pp520-538, 1992.
27. Hirsch JA and Bishop B, Respiratory sinus arrhythmia in humans: how breathing pattern modulates heart rate, Am. J. Physiol. Vol. 241 (Heart Circ. Physiol. 10): H620-H629, 1981.